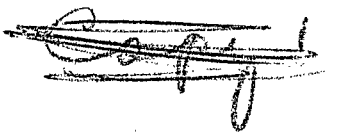

TECHNICAL MEMORANDUM

NATIONAL ADVISORY COMMITTEE FOR AERONAUTICS

No. 1007

KEN

NEW METHOD OF EXTRAPOLATION OF THE RESISTANCE OF A MODEL PLANING BOAT TO FULL SIZE

By W. Sottorf

Luftfahrtforschung
Vol. 16, No. 8, August 20, 1939
Verlag von R. Oldenbourg, München und Berlin

Washington
March 1942

NATIONAL ADVISORY COMMITTEE FOR AERONAUTICS

TECHNICAL MEMORANDUM NO. 1007

NEW METHOD OF EXTRAPOLATION OF THE RESISTANCE OF A MODEL PLANING BOAT TO FULL SIZE[x]

By W. Sottorf

SUMMARY

The previously employed method of extrapolating the total resistance to full size with λ^3 (model scale) and thereby foregoing a separate appraisal of the frictional resistance, was permissible for large models and floats of normal size. But faced by the ever increasing size of aircraft a reexamination of the problem of extrapolation to full size is called for. A method is described by means of which, on the basis of an analysis of tests on planing surfaces, the variation of the wetted surface over the take-off range is analytically obtained. The friction coefficients are read from Prandtl's curve for turbulent boundary layer with laminar approach. With these two values a correction for friction is obtainable.

Worked-out examples indicate that resistance variations analytically determined and those derived from measurements give a practical approximation. A former scale series with the corrections applied to three resistance curves shows good agreement. The step from the 10-ton to the 100-ton flying boat with correction applied is found to be not critical for extrapolation from a model of customary size at the present time.

NOTATION

Model: subscript M

Full size: subscript H

---

[x] "Neues Verfahren der Übertragung des Modellwiderstandes eines Gleitfahrzeuges auf die Hauptausführung." Luftfahrtforschung, vol. 16, no. 8, Aug. 20, 1939, pp. 412-18.

W resistance (kg)

W_N normal resistance (kg)

W_R frictional resistance (kg)

T tangential force (kg)

A hydrodynamic total lift = loading (kg)

G gross weight (kg, ton)

M moment (mkg)

F wetted area (m^2)

F_D pressure area with Vee planing surface (m^2)

Fr Froude number, referred to body length

Fr^* Froude number, referred to a length related to the loading

R Reynolds number

v speed (m/s)

v' speed component (m/s)

l length of wetted area (m)

l_m average length of pressure area with Vee planing surface (m)

b beam of planing surface (m)

b_{St} beam of float at step (m)

b_{nat} natural beam of pressure area with Vee planing surface (m)

q dynamic pressure (kg/m^2)

γ specific weight (kg/m^3)

g acceleration of gravity (m/s^2)

k_s equivalent grain size (cm)

c_f friction coefficient from friction measurements

c_f' friction coefficient of the planing surface

c_α derived lift coefficient of the planing surface

c_B load coefficient

ρ density (kgs^2/m^4)

ν kinematic viscosity (m^2/s)

α angle of attack of the tangent to the horizontal drawn at the point of the step in the center line section (trim)

ϑ angle of dead rise = slope of bottom plating at step to the horizontal (concave Vee type disregarded)

λ model scale

INTRODUCTION

The extrapolation of the resistance of a craft moving on the surface of the water, hence also of a float or hull from model to full size, may be done according to Froude's model method by the following formula

$$\underbrace{W_H}_{\text{total resistance of full size}} = \underbrace{\left(W_M' - c_{f_M} F_M \left(\rho/2\right) v_M^2 \right)}_{\text{frictional resistance of model}} \lambda^3 + \underbrace{c_{f_H} F_H \left(\rho'/2\right) v_H^2}_{\text{frictional resistance of full size}} \quad (1)$$

when temperature and density differences between tank water and sea water are disregarded.

The known factors are: the recorded model resistance W_M, the scale λ, and the density ρ of the water.

Uncertain to define so far were:

1. The coefficient of friction of the model c_{f_M}, according to figure 1, which fluctuates considerably in the low range of Reynolds number depending upon whether the boundary layer is fully turbulent or has laminar approach. On the other hand, the surface of the model may be considered as being technically smooth.

2. The coefficient of friction for full size c_{f_H}, which is affected by roughness, as caused by joints, rivets, or coats of paint, whence manufacturing quality and maintenance condition also assume considerable importance (reference 1).

3. The desired speed affected by the pressure distribution along the planing bottom locally, and the average of which in consequence varies from the forward speed of the float gear v (reference 6).

Unknown factors remain:

4. The size of wetted area F, which changes with speed and trim and whose prediction by test would introduce abnormal complications.

The last reason in particular and the fluctuations in the low range of Reynolds number cited under (1) have led toward the selection of such a great model scale that the results vary from the true values merely within the limits of accuracy customary in such model tests, or within about 5 percent even with disregarded scale effect, that is, by assuming

$$W_H = W_M \lambda^3 \qquad (2)$$

The converted model value is higher than that for full size, hence includes a margin (reference 2).

On the more recently planned giant flying boats, however, (reference 3) the use of correspondingly large models would involve unwanted expense and difficulties in testing, hence the conversion from model of normal size (b_{St} = 0.300 m) (11.8 in.) needs to be reexamined on the basis of improved knowledge. The study is restricted to steady hydrodynamic processes.

NEW METHOD

Figure 2 illustrates in the usual manner the variation of load, resistance, and trim of a 10-ton flying boat as obtained according to the specific method or on the basis of the data from the general towing method (reference 4), and converted to full size by the use of

$$v_H = v_M \lambda^{1/2}$$

$$W_H = W_M \lambda^3$$

$$M_H = M_M \lambda^4$$

For the region of pure planing an investigation of a family of flat rectangular planing surfaces under geometrically similar test conditions has given similitude of pressure areas and moments (reference 5), that is, also similar position of the resultant water force, provided a lower limit of beam of model, located at about b_{St} = 0.150 to 0.200 meter depending on loading, is not exceeded. Thus the application of the foregoing moment conversion affords the same trim for full size and model

$$\alpha_H = \alpha_M$$ [x]

Now, visualize the forebody bottom of the float replaced by a longitudinally straight bottom of constant

---

[x] The subsequent arguments are based on this assumption, although the investigation of float families disclosed also a slight change in the trim with the scale.

beam b_{St} and constant angle of dead rise ϑ corresponding to the main step. Then the normal resistance of this planing surface in region III (fig. 2)

$$W_N = A \tan \alpha \qquad (3)$$

is approximately equal to the normal resistance of the float, if the total resistance is divided in normal and frictional resistance[x]

$$W = W_N + W_R \qquad (4)$$

Hence the variation of the normal resistance W_N conversion of which with λ^3 is justified, can be plotted in figure 2. An extension in the zone of the first hump - zone II - represents merely a rough approximation for W_N, because of the profound effect of the forebody curvature and of the stern. The W_N curve has, however, as is seen, the same character as the converted W_H curve. The formation of the hump is therefore decisively determined by the variation of the trim α. At the start of zone II W_N and W_H are practically coincident, hence the proportion of W_R cannot be considerable (whereby it should be remembered that W_N merely represents an approximation).

The frictional resistance of the substitute bottom is computed with the help of the test data of flat and Vee planing surfaces, for which the frictional coefficients c_f' are known from (reference 5):

$$W_R = W - A \tan \alpha = \frac{T}{\cos \alpha} \cong T = c_f' F q^{y} \qquad (5)$$

But then it is also necessary to insert into the formula as area the wetted area of the float-equivalent planing surface, that is, the area which has the identically derived lift coefficient as the float;

---

[x] The approximation is the closer the more nearly the float bottom ahead of the step resembles a longitudinally straight flat Vee planing surface, as exemplified by the DVL standard float.

[y] At small α, if $N \cong A$.

$$\frac{c_B}{\alpha} = \frac{A}{\alpha\, b^2\, q} \tag{6}$$

This lift coefficient depends only on the aspect ratio l/b and on the Froude number

$$Fr^* = \frac{v}{\sqrt{g\ (A/\gamma)^{1/3}}}$$

The flat planing surface equivalent to the float, in consequence, can be predicted from figure 3.[x] In the event that the pressure area is Vee shaped the procedure is as follows: The size of the pressure area follows similarly to the method for the flat surface; then, with allowance for the angle of dead rise ϑ the calculation proceeds according to

$$\frac{c_B}{\cos\vartheta\ \alpha},\ \frac{l_m}{b} \equiv \frac{l}{b} \quad \text{and} \quad Fr^* = \frac{v}{\sqrt{g\left(\frac{A}{\cos\vartheta\ \gamma}\right)^{1/3}}}$$

The wetted area which in this instance is substantially different from the pressure area is estimated from reference 5 at (fig. 5):

Case 1) loaded width: b, if $\dfrac{\tan\vartheta}{4\tan\alpha} < \dfrac{l_m}{b}$

Case 2) loaded width: $b = b_{nat}$ if $\dfrac{\tan\vartheta}{4\tan\alpha} = \dfrac{l_m}{b}$

$$\left.\begin{aligned} F &= \frac{l\ b}{\cos\vartheta} \\ R &= v\,\frac{l}{b}\,\frac{b}{v}, \text{ wherein } \frac{l}{b} = \frac{l_m}{b} + \frac{\tan\vartheta}{4\tan\alpha} \end{aligned}\right\} \tag{7}$$

---

[x] Obtained from figure 9 of reference 5 after multiplying the derived lift coefficient c_α by l/b.

Case 3) loaded width: b_{nat}, if $\frac{\tan \vartheta}{4 \tan \alpha} > \frac{l_m}{b}$

and $\tan \gamma = \frac{2 l}{b - b_{nat}} \geqq 10.$

Then the insertion of $\frac{l_m}{b_{nat}} = \frac{\tan \vartheta}{4 \tan \alpha}$ gives

$$b_{nat} = \sqrt{\frac{A}{c_\alpha \cos \vartheta \frac{l_m}{b_{nat}} q \alpha}}$$

and

$$l = 2 \frac{l_m}{b_{nat}} b_{nat}$$

hence

$$\left.\begin{aligned} F &= \frac{l (b + b_{nat})}{2 \cos \vartheta} \\ R &= \frac{v l}{\nu} \end{aligned}\right\} \qquad (8)$$

Case 4) loaded width: b_{nat} if $\frac{\tan \vartheta}{4 \tan \alpha} > \frac{l_m}{b}$

and $\tan \gamma = \frac{2 l}{b - b_{nat}} < 10.$

Then:

$$\left.\begin{aligned} F &= \frac{l \left(b_{nat} + \frac{l}{10}\right)}{\cos \vartheta} \\ R &= \frac{v l}{\nu} \end{aligned}\right\} \qquad (9)$$

In cases 1 and 2 the water emerging on the forward contour of the wetted area and passing as plumes along the surface covers almost the whole width of the surface, so that l must be inserted as length in the determination of F and R. In case 3 the limit of spray wetting is approximately indicated by the dashed line, averaged by the solid line. In case 4 an increase in planing surface width puts the edge portions clear of the water. The limit value is $\tan \gamma = 10$.

Since the frictional resistance for the whole take-off run is to be determined, the variation of the wetted area F over the whole speed range is necessary. For several points v in zones II and III the wetted area is computed as before. In addition, the following three values of wetted area (fig. 2) can be plotted for $v = 0$.

F_1 = forebody bottom = greatest possible pressure area is the start of the first curve of wetted area for the equivalent planing surface. This area shows only the slight falling off up to the first hump; while beyond this speed the area, despite the rising dynamic pressure, remains almost constant, because of the decreasing angle of attack, until at around 20 meters per second the angle of attack, kept constant by elevator, has reached $\alpha = 5^\circ$ when the area diminishes rapidly.

Between $F_2 = F_1$ + afterbody wetted area and the end point of zone II the second curve denotes the added wetted afterbody bottom surface, and the third curve indicates the wetted side area, the wetting of which ceases at around 12 meters per second according to flow observations; F_3 represents the total wetted area in rest position.

The second hump speed, which is attributable to added friction at the afterbody bottom surface, occurs when, at high dynamic pressure and low residuary load, the width of the wedge-shaped pressure area originating from the Vee bottom falls short of the width of the float at the step ($b_{nat} < b_{St}$). The proportion of the frictional resistance produced by the pressure area to the total frictional resistance is small shortly before the get-away. This eliminates in general the task of effecting the more cumbersome division of the frictional resistance portions in

the $b_{nat} < b_{St}$ zone. Since in this zone the wetting of the afterbody bottom surface is the cause of the high frictional resistance, we introduce one-third of the afterbody bottom surface; and for the determination of the Reynolds number $\frac{v\,l}{\nu}$ we put one-third of the afterbody length from main step to second step with corresponding change from v_{min} and extending to $v_{take\text{-}off}$. This measure is to be considered as an expedient, for the wetting of the afterbody area subject to the spray water effect is physically unlike the wetting of a pressure area. Unknown quantities remain the actual surface dimensions, the density of wetting, and the rate of spray impact. However, since only the difference of the friction coefficients of model and full size is involved in the conversion process, the error is presumably allowable.

In the range of the first hump the total residuary resistance exceeding the analytically defined frictional resistance is interpreted as normal resistance, because in this instance, as already stated, the forebody curvature and afterbody effect cause a discrepancy between analytically defined and true normal resistance. To determine the frictional resistance the partial areas F_1, F_2, and F_3 are therefore combined to obtain the interpolated total wetted area F, whereby assuming

$$l = \frac{F \cos \vartheta}{b_{St}}$$

Following the determination of the area to be entered in equation (5) for the frictional resistance, the sole lacking c_f' value is read from Prandtl's curve for turbulent boundary layer with laminar approach (fig. 1).

$$c_f = \frac{0.455}{(\log R)^{2.58}} - \frac{1700}{R}$$

which, according to reference 5, covered all planing surface experiments satisfactorily.[x]

---

[x]The following exceptional case is cited: too small a model ($b_{St} \leqq 0.15$ m) is unsuitable for exploration of the

(Continued on p. 11)

The W_R curve for full size with implicit maximums and the curve of the analytical total resistance as the sum $W = W_N + W_R$ is obtained in this manner, the difference of which with respect to the W_H curve converted after measurement is due to the scale effect - provided it fully corresponds to the actual resistance.

Having thus established the similarity of the numerically defined and the converted total resistance throughout the take-off range considered, the correction can be applied.

As correction for the friction

$$\left(c_{f_M} - c_{f_H}\right) F_H \frac{\rho}{2} v_H^2 \qquad (10)$$

is to be deducted according to equation (1). The Reynolds number for full size is according to the model law

$$R_H = R_M \lambda^{3/2} \qquad (11)$$

In figure 4 the correction factor $\left(c_{f_M} - c_{f_H}\right)$ is plotted against $R_M = \frac{v_M l_M}{\nu}$ with λ as parameter.

The reduced W_H curve, also shown in figure 2, is almost coincident with the theoretical W-curve in the region of pure planing as expected.

(Continued from p. 10)

first hump because of anticipated dissimilarity of flow condition, although it can be used under certain circumstances in the region of pure planing and in the region preceding get-away. Then, however, the Reynolds numbers become so small, as a result of the small dimensions, that they generally fall in the range $R_M < 3\ 10^6$, where the discrepancies between $c_{f_{turbulent}}$ and $c_{f_{laminar-turbulent}}$ are unusually great. Since the afterbody wetting before get-away is the chief cause of the high resistance and hence precludes any laminar entrance of

(Continued on p. 12)

EFFECT OF ROUGHNESS

Figure 6 was taken from reference 7 which deals with scale experiments over the whole speed range inclusive of full size. An unexpected departure is noticed in the upper speed range, where the full-scale resistance exceeds the converted model resistance. The higher resistance is attributed to the effect of rivet heads and laps, although no analysis is given.

The increase in roughness (figure 1) for the full size can be defined according to Schlichting (reference 1) if the equivalent grain size k_s resembling its surface condition is experimentally ascertained. Since Göttingen reports on systematic tests with plate roughness, such as occurs on the bottom of a float, are available, the least roughness of Schlichting's study and the grain size to which the tests refer will be checked by a rough calculation.

By way of example let the surface length be $l = 1$ m and the speed $v = 30$ m/s, which is a condition before get-away. With $\nu = 1.3 \times 10^{-6}$ m^2/s we get $R = 2.3 \times 10^7$ and for it

$$c_{f_{smooth}} = 0.00266$$

The least roughness was observed on plates with spherical segments resembling flat rivet heads of 2.6-millimeter height and 8-millimeter diameter spaced at 40 millimeters over the surface (plate XIII, $k_s = 0.059$ cm). The relative roughness is $l/k_s = 3.23 \times 10^3$ and hence

---

(Continued from p. 11)

the boundary layer, it is justified to effect the correction for friction in such a case on the basis of the turbulent boundary layer curve

$$c_f = \frac{0.455}{(\log R)^{2.58}}$$

as confirmed by the close agreement between measurement and conversion on two similar models 0.15 and 0.3 m width (not included herein).

$c_{f_{rough}} = 0.0063$, that is, 137-percent-roughness increase.

The roughness produced by sand of 1.35-millimeter average grain size on the varnished surface has with

$k_s = 0.222$ centimeter at $\frac{l}{k_s} = 4.5 \times 10^2$ a

$c_{f_{rough}} = 0.0106$, that is, 300-percent-roughness increase, from which the profound effect of roughness at high planing speeds becomes apparent.

In a check test on a standard model float of 0.3-meter beam, the results of which are reproduced in figure 7, a quantitative check on the model was made, particularly respecting the potential resistance increase prior to lift-off due to the effect of spray water on the afterbody bottom area.

The upper half of the diagram shows under a constant 50-kilogram load the planing number of the first hump $\epsilon = \frac{W_{max}}{A}$ plotted against the trim α for three model conditions: smooth model, afterbody bottom roughened by coat of sand of 1.35-millimeter grain size, and the whole bottom roughened.

It is seen that afterbody roughness alone has practically no effect, since at the first hump only the extreme tip of the afterbody is loaded. The effect of forebody roughness is, on the other hand, considerable. The resistance increase is greatest at small α because of the greater wetted area; at $\alpha = 9.5^\circ$ as expected at the hump, the increase amounts to 41 percent.

The lower half of the diagram shows the condition shortly before lift-off at a 10-kilogram load and 15.5 meters per second speed. The three afore-mentioned model conditions are now augmented by a fourth, forebody alone smooth. Here the increased resistance caused by afterbody spray with increasing α over the condition forebody alone, is plainly apparent. While the increase in total resistance due to roughness of afterbody rises by 115 percent at $\alpha = 9.5^\circ$ - the greatest angle obtainable for early lift-off - this percentage of roughness even of the forebody is only 50 percent.

Inserting one-third of the afterbody surface and one-third of the afterbody length for computing the factor c_f as suggested in the present report, gives according to Schlichting a $c_{f_{rough}}$ of 0.015. The same value is obtained from the measurement at $\alpha = 9.5^\circ$. On the smooth model agreement between theory and test prevails at $\alpha = 7.5^\circ$. In other words, the assumptions regarding size and length of wetted afterbody bottom area are confirmed at the high trims aimed at for purposes of quick get-away.

So, even though the correction dealt with in the present report yields in the zone of the second hump a deduction, full attention should be given to the fact that resistance increases attributable to roughness effect can materially impair the get-away power of highly loaded seaplanes.[x]

RECAPITULATION OF CONVERSION METHOD

1. $W_H = W_M \lambda^3$, A^* and α are plotted against α.

2. $W_{max\ I}$, $W_{max\ II}$, and W_{min} are marked.

3. Zone III, condition of pure planing, is restricted on the basis of flow observations (in general close up to $v_{max\ I}$ to v_{min}).

4. $\frac{v_{max\ I}}{2}$ is chosen as origin of the ordinate, v_{start} as the final ordinate.

5. The equivalent pressure area F_D and the wetted area F of the planing surface are determined for about three points in zone III, pure planing, and one point at $v_{max\ I}$. The angle of dead rise β of the planing surface hereby corresponds to the angle of

[x]Parkinson arrives at the same conclusion in an article (reference 9) published while the present report was being printed, wherein, on the basis of a study on a model fitted with rivet heads, the increase due to roughness of lower roughness density is defined accordingly - lower (40 percent).

dead rise of the float bottom at the first step with no allowance for concave Vee planing bottom at the bow. With the inclusion of the three initial points at $v = 0$ and of the end point at v_{start} F can be plotted with respect to v.

6. One-third of the afterbody bottom area is assumed as area in zone IV in the central third of this zone, while at either side the decrease to the predetermined area is linear.

7. For the determination of the Reynolds number the length of the equivalent wetted area

$$l = \frac{F \cos \vartheta}{b_{St}}$$

serves as length l in zones II and III, and one-third of the length of the afterbody from main step to the second step in the central third of zone IV rectilinearly decreasing to the adjoining junction point and to zero, respectively.

8. The correction is applied according to equation (10) and deducted from W_H.

EXAMPLES OF CONVERSIONS

To identify the effect of increasing gross weight on the scale effect the conversion of the example for figure 2 to 100-ton gross weight is carried out in figure 8 where W/G is plotted nondimensionally as $f(Fr)$ to $G_M = 60$ kilograms and $G_H = 10$ tons in comparison. It is seen - especially in the separate plot of the friction correction for 10 and 100 tons - that the correction is subject to a relatively small increase during the jump from 10 to 100-ton gross weight.

One of Schmidt's (reference 8) scale investigations with models at scale $\lambda = 5$ and $2\frac{1}{2}$ and full-size measured on an experimental airplane is reproduced in figure 9, showing the resistance with and without correction for

friction and the trim with a slight dependence on the scale. The applied correction brings the results of model and full size in good agreement.

Translation by J. Vanier,
National Advisory Committee
for Aeronautics.

REFERENCES

1. Schlichting, H.: Experimental Investigation of the Problem of Surface Roughness. T.M. No. 823, NACA, 1937.

2. Sottorf, Walter: Über den Einfluss des Modellmassstabes bei der Untersuchung von Flugzeugschwimmern. 2. Flugtechn. Bd. 22, Heft 24, 1932. TM 704 ?

3. Sikorsky, I. I.: Das Grossflugboot. Jahrb. 1938 der deutschen Luftfahrtforschung. Ergänzungsband p. 11.

4. Sottorf, Walter: The Design of Floats. T.M. No. 860, NACA, 1938.

5. Sottorf, Walter: Analyse experimenteller Untersuchungen über der deutschen Luftfahrtforschung, 1937, p. I 320 and Werft-Reed.-Hafen, Heft 5/6, 1938. TM 1061

6. Sottorf, Walter: Versuche mit Gleitflächen, Pt. III. Werft-Reed.-Hafen, Heft 4/5, 1938.

7. Hanson, J.: Full Scale Water Resistance of the Singapore II C in Steady Motion. R.& M. No. 1805, British A.R.C., 1936.

8. Schmidt, Rudolph: The Scale Effect in Towing Tests with Airplane-Float Systems. T.M. No. 826, NACA, 1937.

9. Parkinson, J. B.: Tank Tests to Show the Effect of Rivet Heads on the Water Performance of a Seaplane Float. T.N. No. 657, NACA, 1938.

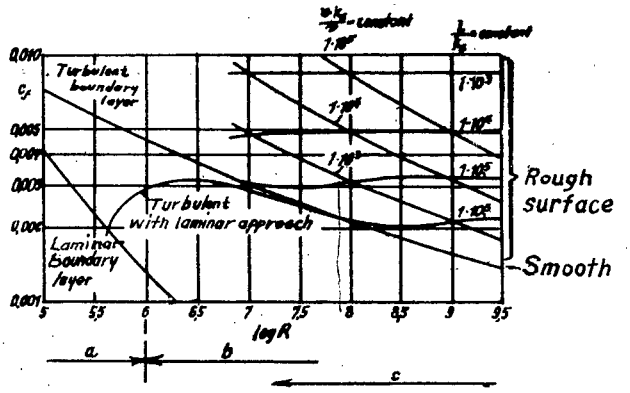

Figure 1.- Coefficient of friction c_f plotted against Reynolds number $\frac{Vk}{\nu}$ for different boundary layer conditions and relative roughness $\frac{k}{k_s}$ (k_s = equivalent grain size) according to Schlichting. (ref. 1) (a) Zone unsuitable because of too small model size and time of effect of surface tension. (b) Model range with normal model size. (c) Full scale range.

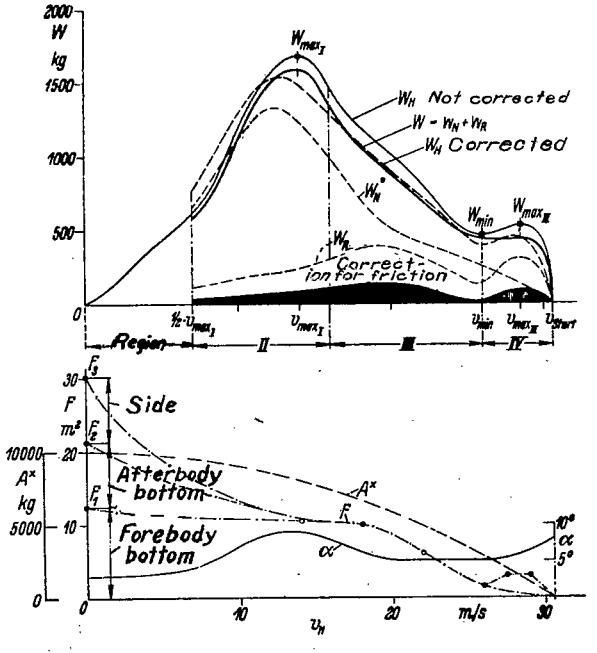

Figure 2.- Division of resistance, identification of areas and correction for friction on a flying boat of

$$G = 10000 \text{ kg}, \quad b_{St} = 1{,}65 \text{ m},$$

$$\frac{l_L}{b_{St}} = 9{,}19, \quad \varphi = 20^\circ, \quad \lambda = 5{,}5.$$

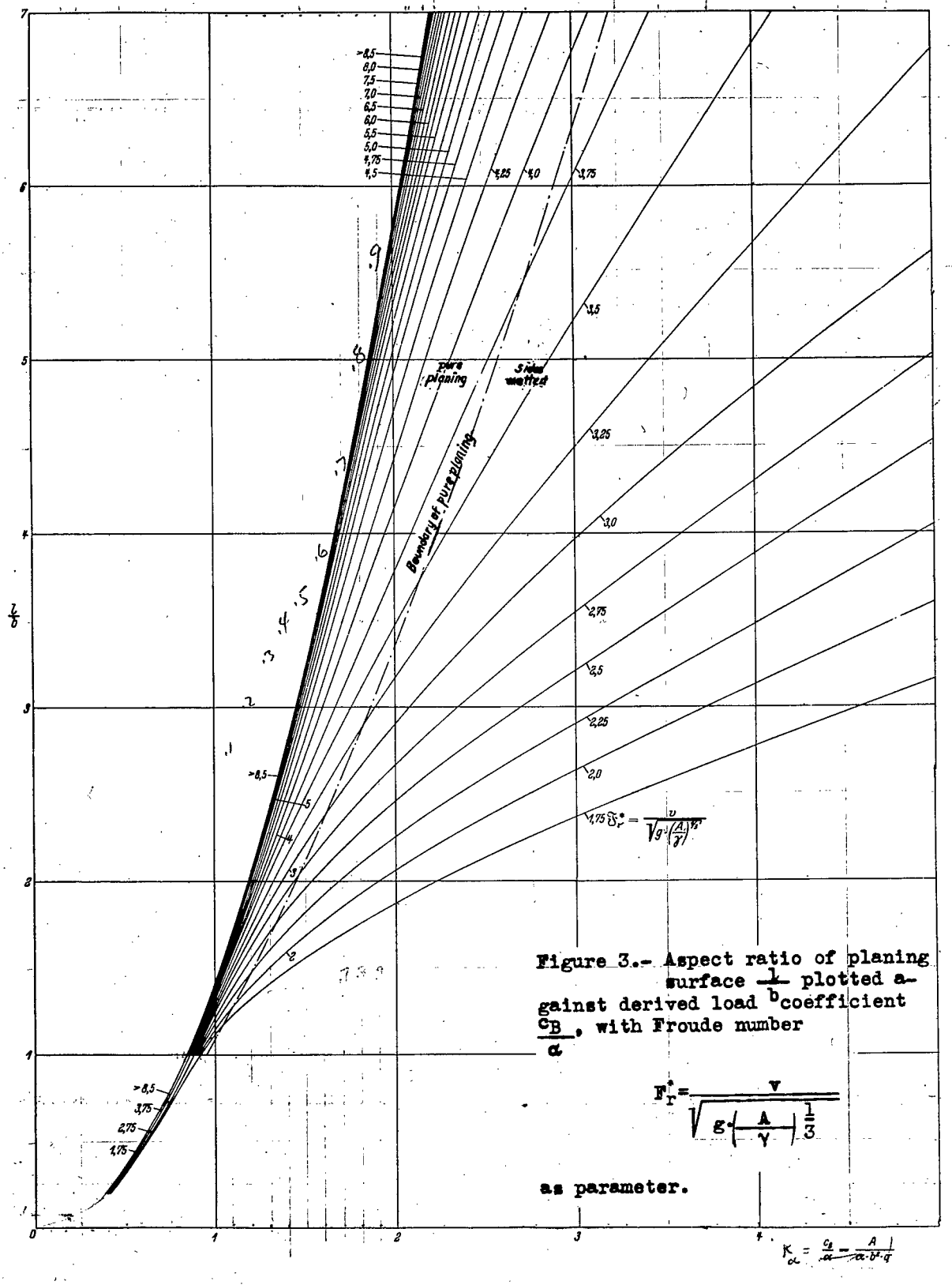

Figure 3.- Aspect ratio of planing surface $\frac{l}{b}$ plotted against derived load coefficient $\frac{c_B}{\alpha}$, with Froude number

$$F_r^* = \frac{V}{\sqrt{g \sqrt[3]{\frac{A}{\gamma}}}}$$

as parameter.

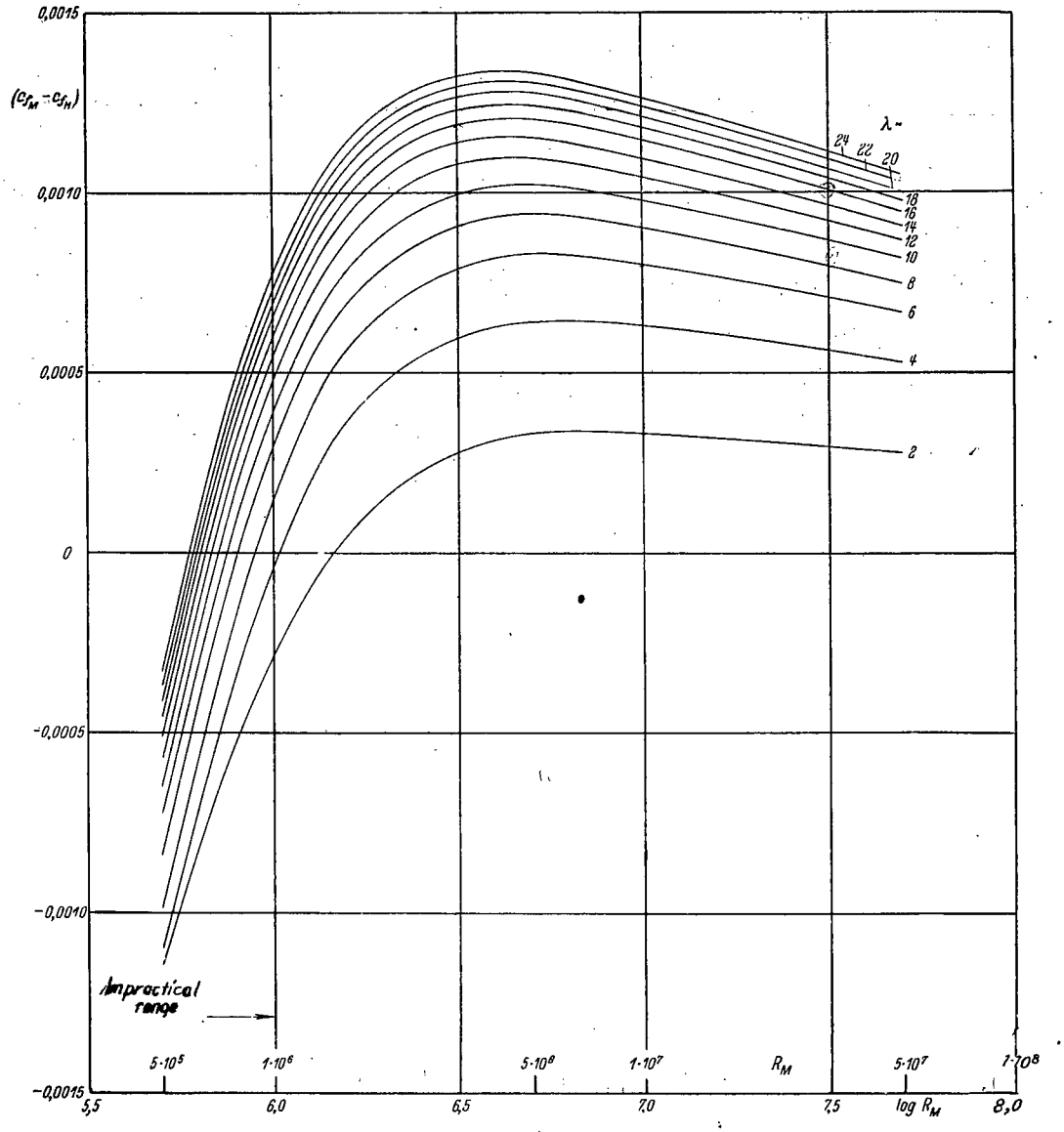

Figure 4.- Correction factor ($cf_M - cf_H$) plotted against model Reynolds number R_m with scale λ as parameter.

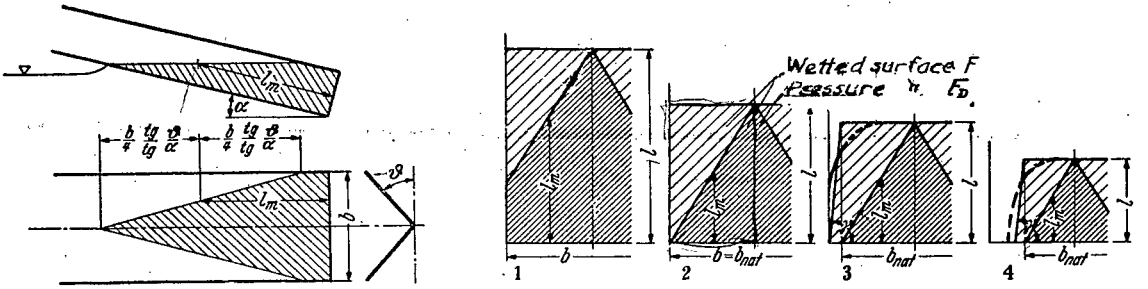

Figure 5.- Pressure area and wetted area on vee type planing surface.

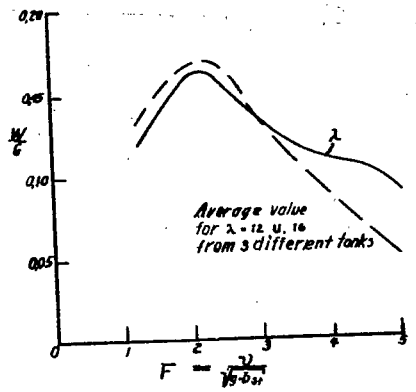

Figure 6.- Data from English scale tests with the Singapore II C.

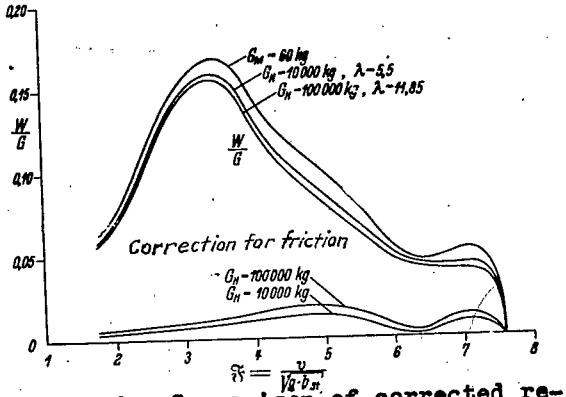

Figure 8.- Comparison of corrected resistance curves of a flying boat on raising the gross weight from 10 to 100 tons.

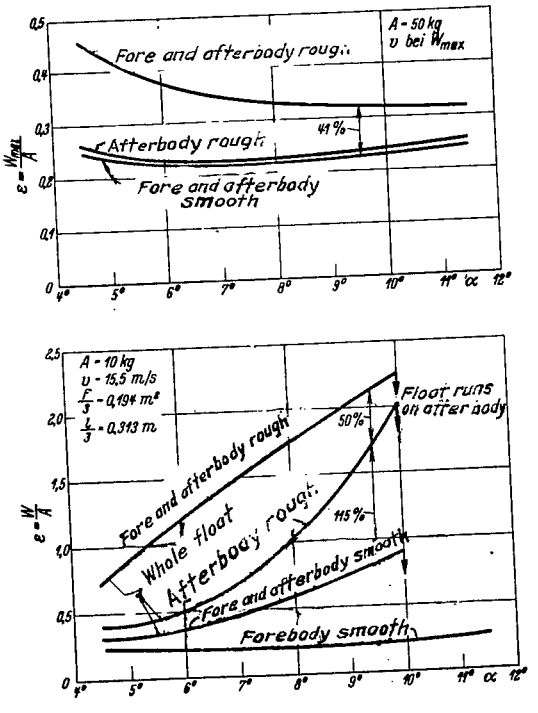

Figure 7.- Effect of roughness on the resistance of a model float 0,3 m beam at hump speed and before get away.

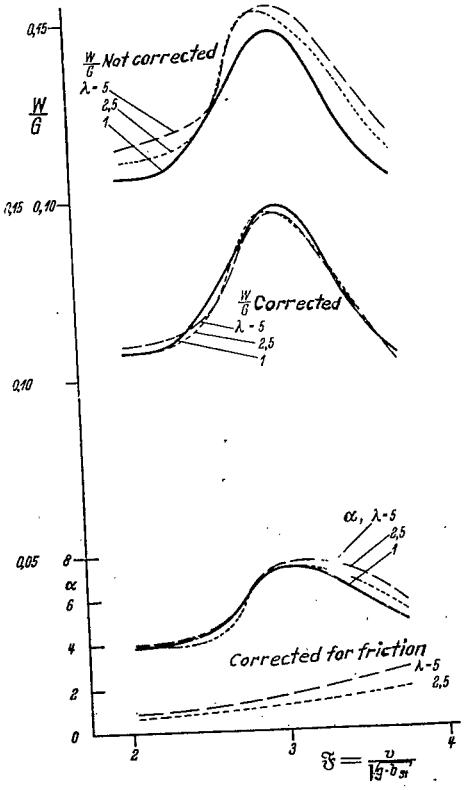

Figure 9.- Correction of a resistance curve ascertained with full scale "III" and two models from Schmidt's scale series.